

# Stochastic switching in systems with rare and hidden attractors

Nataliya Stankevich<sup>1,2,a</sup>, Erik Mosekilde<sup>3</sup>, and Aneta Koseska<sup>4</sup>

<sup>1</sup> Department of Applied Cybernetics, St. Petersburg State University, Saint-Petersburg, Russia

<sup>2</sup> Department of Radio-Electronics and Telecommunications, Yuri Gagarin State Technical University of Saratov, Saratov, Russia

<sup>3</sup> Department of Physics, The Technical University of Denmark, Lyngby, Denmark

<sup>4</sup> Department of Systemic Cell Biology, Max Planck Institute of Molecular Physiology, Dortmund, Germany

**Abstract.** Complex biochemical networks are commonly characterised by the coexistence of multiple stable attractors. This endows living systems with plasticity in responses under changing external conditions, thereby enhancing their probability for survival. However, the type of such attractors as well as their positioning can hinder the likelihood to randomly visit these areas in phase space, thereby effectively decreasing the level of multistability in the system. Using a model based on the Hodgkin-Huxley formalism with bistability between a silent state, which is a rare attractor, and oscillatory bursting attractor, we demonstrate that the noise-induced switching between these two stable attractors depends on the structure of the phase space and the disposition of the coexisting attractors to each other.

## 1 Introduction

Multistability is a universal, essentially nonlinear aspect of matter and its organization from molecular arrangements and chemical reactions to multistability in the behavior, phenotype etc. [1], [2], [3], [4], [5]. This reflects the coexistence of stable states or attractors in parameter space. The stability of these states on the other hand depends on how quickly the system returns to a state following a perturbation. For example, in gene regulatory networks, the coexistence of multiple coexisting attractors (i.e. oscillations and steady states) has been associated with the existence of stable phenotypes and the probability for survival [6], [7], cell decision during cellular differentiation [8], [9], [10] etc. Particularly notable is for example the pronounced multistability in excitable systems, such as systems describing neuronal dynamics [11], [12], [13], [14], [15], [16]. It has been proposed that in neuronal systems for example, multistability can play functional roles in short-term memory and maintaining posture. Particularly interesting in these class is the mechanisms supporting multistability of bursting regimes, which are not well understood or classified. Bursting dynamics on the other hand is widespread in various biophysical processes, typical

---

<sup>a</sup> e-mail: stankevichnv@mail.ru

not only for neurons, but also pancreatic beta-cells, cardiac cells, etc. [17], [18]. Bursting activity is the result of an interplay of ionic currents which are voltage-gated on various timescales, very commonly captured through the Hodgkin-Huxley formalism [19].

However, how often the stochastic system will visit distinct areas in phase space where a particular attractor is situated depends on the type of the attractors, their basin, as well as their relative positioning towards each other. For example, if the basin of attraction of stable states are very small in comparison with the basins of other coexisting attractors in the system, they will not be very sensitive towards noise and system parameters so a sudden shift to such a regime is less likely to occur [20], [21]. If on the other hand, the basins of attraction of a specific attractor does not touch unstable fixed points (if they exist) and are located far away from such points, they are called hidden attractors [22]. Recently, it has been shown that multistability is connected with the occurrence of these unpredictable hidden attractors [23]. Numerical localization, especially of the hidden attractors is not straightforward since there are no transient processes leading to them from the neighborhoods of unstable fixed points and one has to use special analytical-numerical procedures [22]. However, the identification of hidden attractors is the major issue from aspect of applications since the knowledge about the emergence and properties of hidden attractors can increase the likelihood that the system will remain on the most desirable attractor and reduce the risk of the sudden jump to undesired behavior. This is particularly important for biophysical and biochemical systems, since these processes are inherently noisy due to small number of molecules or external perturbations [25], [26]. The relationship between hidden attractors and multistability [23], as well as for the rare attractors [27] has been shown mainly for nonlinear dynamics models such as the Chua system, van der Pol oscillator, etc., whereas the investigations of this problem in the context of biophysical models is relatively limited [28].

Thus, in the present work we consider models of neuronal dynamics that exhibit bistability between silent and bursting state. We particularly focus on the case when the coexisting dynamical regimes are unequal, such as the silent state is a rare, and bursting state is a hidden, or a self-excited attractor, and investigate the conditions leading to noise-induced switching.

## 2 Hodgkin-Huxley-like models with rare and hidden attractors

In the current section we describe two models in which bistability between silent and bursting state is described. Based on sufficient generalization, it can be assumed that for this type of bistability the basin of attraction of the stable equilibrium should be small in respect to basin of attraction of the bursting attractor. This is due to the fact that the equilibrium state is located on the intersection of the fast and the slow manifolds of the system, whereas at the same time, the bursting attractor is located on a part of the branch of the fast-manifold. Thus, the coexisting equilibrium state should be situated beside or inside of the bursting attractor. In this way, the basin of attraction of the silent state will be small, rendering the stable steady state as a rare attractor.

### 2.1 Model of a leech neuron

As the first example of the model that displays bistability between silent and bursting states, we consider a model of leech neuron, which was suggested in [12]. The simplified

**Table 1.** Parameters of the model (1).

$C =$	0.5	$\tau_h =$	0.0405 Sec		
$g_{Na} =$	250	$g_{CaS} =$	80	$g_{leak} =$	15.362
$V_{Na} =$	0.045 V	$V_{CaS} =$	0.135 V	$V_{leak} =$	-0.0502 V
$B_h =$	0.031 V	$B_{hCaS} =$	0.06 V		

leech neuron model is described by the following equations:

$$\begin{aligned}
C\dot{V} &= -I_{Na}(V, h_{Na}) - I_{CaS}(V, h_{CaS}, m_{CaS}) - I_{leak}(V), \\
\tau_h \dot{h}_{Na} &= f_\infty(500, B_h, V) - h_{Na}, \\
\tau_{mCaS} \dot{m}_{CaS} &= f_\infty(-420, 0.0472, V) - m_{CaS}, \\
\tau_{hCaS} \dot{h}_{CaS} &= f_\infty(360, B_{hCaS}, V) - h_{CaS}.
\end{aligned} \tag{1}$$

Here  $V$  represents the membrane potential of the cell, the functions  $I_{Na}$ ,  $I_{CaS}$ ,  $I_{leak}$  define three intrinsic currents of the system: the fast sodium  $I_{Na}$ , the slow calcium  $I_{CaS}$  voltage-dependent currents:

$$I_{Na}(V, h_{Na}) = g_{Na} f_\infty^3(-150, 0.028, V) h_{Na} (V - V_{Na}), \tag{2}$$

$$I_{CaS}(V, h_{CaS}, m_{CaS}) = g_{CaS} m_{CaS}^2 h_{CaS} (V - V_{CaS}), \tag{3}$$

and the leak current

$$I_{leak}(V) = g_{leak} (V - V_{leak}). \tag{4}$$

The description of the model parameters (1) as well as their physiological relevance are given in details in [12]. Shortly, the function  $f_\infty(A, B, V)$  is a steady-state activation (inactivation) function of a voltage-gated ionic current given by the sigmoidal function:

$$f_\infty(A, B, V) = \frac{1}{1 + e^{A(V+B)}}. \tag{5}$$

Here  $B$  is the half-activation (half-inactivation) membrane potential at which  $f_\infty = 0.5$ . The voltage-dependent time constants for the activation and inactivation variables of the calcium current, following to [12], we take from [29]:

$$\tau_{mCaS} = 0.005 + 0.134 f_\infty(-400, 0.0487, V),$$

$$\tau_{hCaS} = 0.2 + 5.25 f_\infty(-250, 0.043, V).$$

One can see that the inactivation of the calcium current,  $h_{CaS}$ , is the slowest variable in the model (1), whereas the voltage on the membrane  $V$  represents the fastest variable.

In [12], areas of coexistence between bursting and silent regimes in the parameter plane ( $g_{leak}$ ,  $V_{leak}$ ) have been determined. By fixing the parameters inside the noted area of bistability, we can estimate the structure of phase space in this parameter region.

For parameters, defined in table 1 the model (1) has three equilibrium points:

$$EP^1 = (V^{01}, h_{Na}^{01}, m_{CaS}^{01}, h_{CaS}^{01}) = (-47.798, 0.99977, 0.43752, 0.012216),$$

$$EP^2 = (V^{02}, h_{Na}^{02}, m_{CaS}^{02}, h_{CaS}^{02}) = (-36.326, 0.93481, 0.98972, 0.00019887),$$

$$EP^3 = (V^{03}, h_{Na}^{03}, m_{CaS}^{03}, h_{CaS}^{03}) = (-27.237, 0.13223, 0.99977, 0.0000075).$$

The first of them  $EP^1$  is stable, and the second  $EP^2$  and the third  $EP^3$  are unstable. In order to visualize coexisting dynamical regimes we construct their basins of

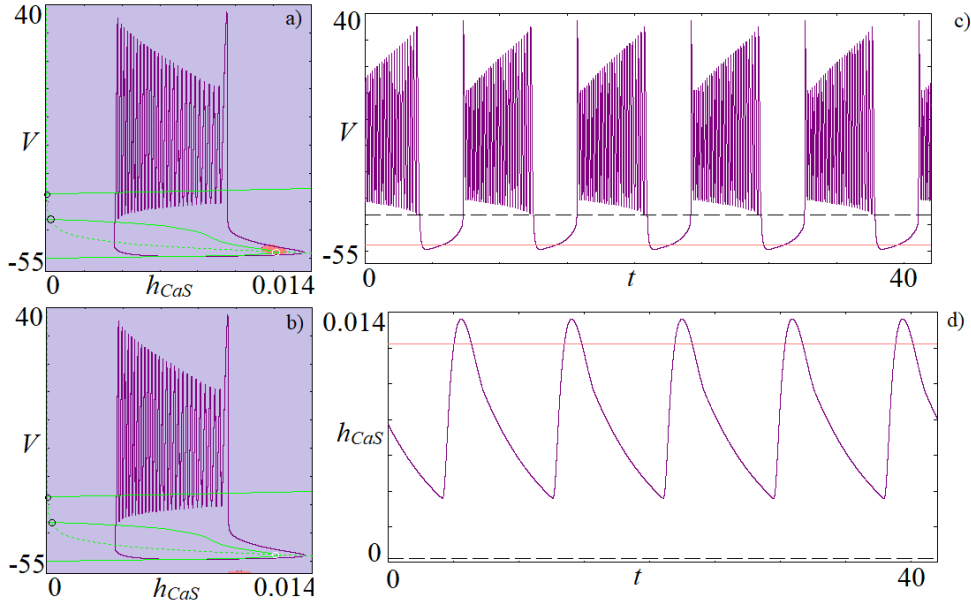


**Fig. 1.** a) and b) fast and slow manifolds (green solid and dot lines), 2D-projection of the bursting attractors (purple line) and equilibrium points (black and white circles with respect to the unstable and stable equilibria). The basins of attractions of the coexisting attractors are shown with red (basin of attraction of stable equilibrium point) and light violet color (basin of attraction of the bursting attractor). c) and d) Representative time series of the fast and slow variables of the system for the coexisting dynamical regimes; phase trajectory is purple, stable equilibrium  $EP^1$  is red line and unstable equilibrium  $EP^2$  is dashed black line. All parameters correspond to Table 1.

attraction and analyze two-dimensional cross-sections in the vicinity of each equilibrium point. In Fig. 1 a) and b), the corresponding planes for varying initial conditions are shown. Fig. 1 a) corresponds to the initial conditions in the vicinity of the stable equilibrium, whereas the initial conditions of the other two variables,  $h_{Na}$  and  $m_{CaS}$ , were fixed exactly at the equilibrium point  $EP^1$ . On the other hand, Fig. 1 b) corresponds to the vicinity of unstable equilibrium  $EP^2$ . From Fig. 1 a) it can be seen that the largest portion of the plane is occupied by the basin of attraction of bursting attractor. Within this basin of attraction however, the basin of the stable equilibrium is represented with a relatively small area, located in the vicinity of unstable point  $EP^2$ . The structure of the basins of attraction in the vicinity of unstable equilibrium  $EP^3$  is the same as Fig. 1 b). Thus, starting from the vicinity of stable equilibrium  $EP^1$ , the trajectory in phase space evolves towards the equilibrium point, whereas when starting in the vicinity of unstable equilibria  $EP^2$  and  $EP^3$ , the phase-space trajectory asymptotically converges to the bursting attractor (Fig. 1 a) and b)). This indicates that the coexisting attractor is self-excited. Thus, if the transient starts from randomly distributed initial conditions inside a cube in phase space that covers both attractors ( $V_0[-55 - 40]$ ,  $h_{Na}[0 - 1.05]$ ,  $m_{CaS}[0.2 - 1.05]$ ,  $h_{CaS}[0 - 0.014]$ ), then the probability to reach the stable equilibrium point approximates 1.11%, rendering the random "finishing" of this attractor a rare event. This probability of course scales with the size of the cube: increasing the size will conversely decrease this probability. The stable equilibrium point  $EP^1$  can therefore be classified as a rare attractor. Moreover, as depicted by the time series of fast and slow dynamical variables,  $V$  and

**Table 2.** Relevant parameters for the model (6).

$\tau =$	0.02 Sec	$\tau_S =$	35 Sec	$\sigma =$	0.93		
$g_{Ca} =$	3.6	$g_K =$	10.0	$g_S =$	4.0	$g_{K2} =$	0.2
$V_{Ca} =$	25.0 mV	$V_K =$	-75 mV				
$\theta_m =$	12.0 mV	$\theta_n =$	5.6 mV	$\theta_S =$	10.0 mV	$\theta_p =$	1 mV
$V_m =$	-20.0 mV	$V_n =$	16.0 mV	$V_S =$	-35 mV	$V_p =$	47 mV

$h_{CaS}$ , in Figs. 1 c) and d), the stable equilibrium and the bursting attractor display intersection in these projections.

## 2.2 A modified Sherman model

We next consider a modification of the model suggested by Sherman and Rinzel [17] that describes the calcium dynamics of the beta-cells. The modifications introduced in [28] ensure a coexistence between bursting and silent states. This modified Sherman model has the form:

$$\begin{aligned}\tau\dot{V} &= -I_{Ca}(V) - I_K(V, n) - I_{K2}(V) - I_S(V, S), \\ \tau\dot{n} &= \sigma(f_\infty(V_n, \theta_n, V) - n), \\ \tau_S\dot{S} &= f_\infty(V_S, \theta_S, V) - S.\end{aligned}\quad (6)$$

Here,  $V$  also represents the membrane potential of the cell,  $n$  is the fraction of open voltage-gated  $K^+$ -ion channels, whereas the functions  $I_{Ca}(V)$ ,  $I_K(V, n)$  define two intrinsic currents, the fast calcium  $I_{Ca}$  and the fast potassium  $I_K$  currents:

$$I_{Ca}(V) = g_{Ca}f_\infty(V_m, \theta_m, V)(V - V_{Ca}), \quad (7)$$

$$I_K(V, n) = g_K n(V - V_K), \quad (8)$$

$S$  is the fraction of open voltage-gated  $Ca^{2+}$ -ion channels, which directly acts on the concentration of  $Ca^{2+}$ . The third current  $I_S(V, S)$  is a  $Ca^{2+}$ -sensitive slow potassium current, which is directly activated by  $Ca^{2+}$ .

$$I_S(V, S) = g_S S(V - V_K), \quad (9)$$

The gating variables for  $n$  and  $S$  are the opening probabilities of the fast and slow potassium currents described by the sigmoidal function (5).

Thus, this modified beta-cell model has the new potassium current is the form:

$$I_{K2}(V) = g_{K2}p_\infty(\theta_p, V_p, V)(V - V_K), \quad (10)$$

where

$$p_\infty(A, B, V) = \frac{1}{e^{A(V+B)} + e^{-A(V+B)}}. \quad (11)$$

It has been shown that in a certain parameter interval, coexistence between the bursting attractor and stable equilibrium point is possible [28] and corresponding parameters in Table 2 are presented.

In this parameter range, the model (6) has one stable equilibrium point  $(V_0, n_0, S_0) = (-49.084, 0.0027105, 0.19648)$ . In Fig. 2 examples of the coexisting attractors are presented. In Fig. 2 a) the fast-slow manifolds, the projection of the bursting attractor and its basin of attraction of the modified model (6) are shown. The basin of attraction in this case was constructed using Poincaré section for the  $n = 0.02$  plane,

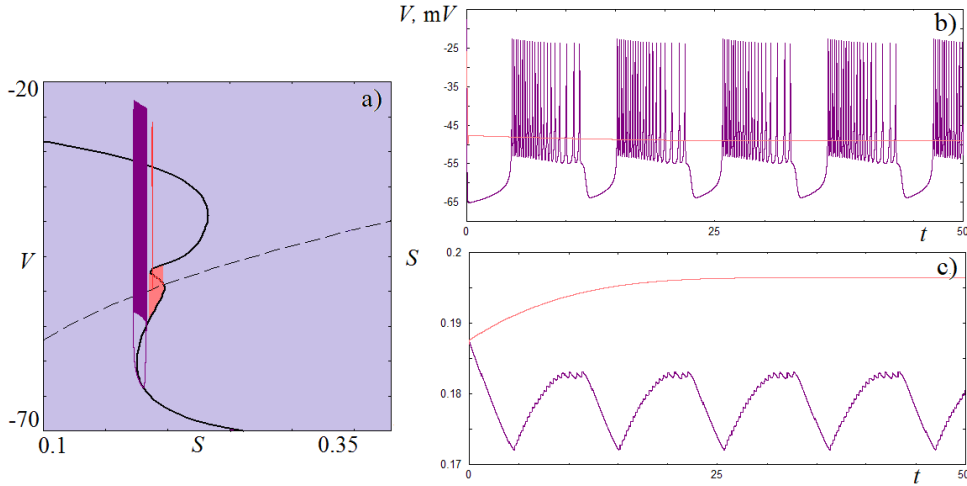


**Fig. 2.** a) fast and slow manifolds (solid and dashed black lines, respectively), 2D-projection of coexisting the bursting attractor (purple line) and silent state (red trajectory goes to equilibrium) with their basins of attraction; b) and c) time series of coexisting regimes (red trajectory starts from the basin of the stable equilibrium, purple trajectory starts from the basin of the bursting attractor).  $V_p = -47$  mV,  $g_{K2} = 0.2$ .

and initial condition of the third variable  $n$  was chosen exactly at the equilibrium point,  $n_0 = 0.00275$ . The characteristic  $S$ -form of the fast manifold has an additional bending in which the equilibrium point of the system becomes stable (Fig. 2 a)). This bending in turn determines the basin of attraction of the equilibrium stable point (red color). Outside of this area, the basin of attraction of the bursting attractors is present (purple area). Since the area of attraction of the stable equilibrium point is very small, we can infer that this attractor is a rare attractor. If we again take randomly distributed initial conditions inside a predefined cube in phase space, which covers both attractors ( $V_0[-65--20]$ ,  $n_0[0-0.12]$ ,  $S_0[0.17-0.2]$ ), then the probability of realization of the stable equilibrium point in this case equals 5.5%. Starting from the vicinity of the single equilibrium point, however, it is possible to reach only this equilibrium (Fig. 2 a)). This in turn allows us to conclude that the bursting attractor is hidden in this case.

### 3 Noise-induced switching in multistable systems with rare and hidden attractors

We next study the influence of noise on the dynamics of these systems when bistability between bursting oscillatory regime and stable steady state is present. Generalized Hodgkin-Huxley-type of model with noise can be written in the form:

$$\dot{V} = F(V, \dots) + \sqrt{2D}n(t) = \sum_i I_i/\tau + \sqrt{2D}n(t), \quad (12)$$

where  $n(t)$  depicts an additive noise source, which is a Gaussian white noise with zero mean and  $D$  is the noise intensity. In Hodgkin-Huxley-type of models the noise necessarily mimics fluctuations of the membrane voltage, and not the probability of opening of the ion channels and is therefore commonly added to the first equation.

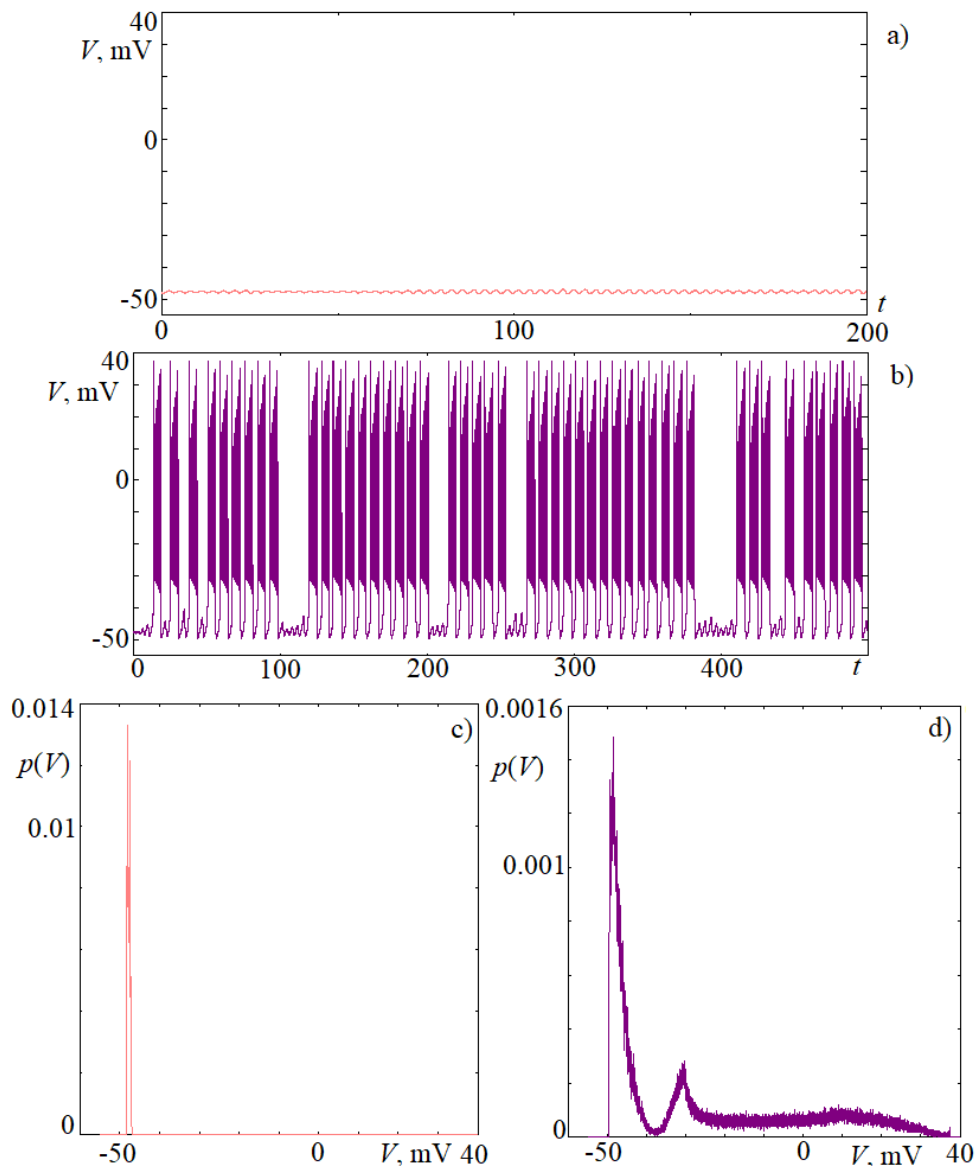


**Fig. 3.** a) and b) Time series of the fast variable  $V$ , and the corresponding c) and d) stationary distribution for model (1) with and different noise intensity: a), c)  $D = 0.005$ ; b), d)  $D = 0.245$ .

It is well-known that in multistable system, switching between coexisting attractors can be observed for certain noise levels [9], [20], [21], [30]. The previously described system thus make an interesting case study, given that the attractors are rare or hidden, and the dynamics of the system in the presence of noise is non-intuitive<sup>1</sup>. We thus first consider the leech neuron model (1), where the coexistence between a rare stable steady state and bursting attractor was observed. For initial condi-

<sup>1</sup> We can notice recent paper [24] where hidden attractors in the present of noise are studied.

tions exactly at the stable equilibrium point and small noise intensities (Fig. 3 a), c),  $D = 0.005$ ), the system does not leave the rare attractor and correspondingly, the stationary distribution has only one maximum situated in the vicinity of stable equilibrium point  $EP^1$ . Thus, the phase trajectory is fluctuating in the vicinity of the stable point. When the noise intensity is sufficiently increased (Fig. 3 b), d),  $D = 0.245$ ), the dynamics of the system switches between the rare stable equilibrium and the bursting oscillations. This in turn corresponds to a bimodal distribution: even though the minor peak corresponds to the trapping of the trajectory in the bursting attractor, the major peak that represents the persistence of the phase space trajectory in the vicinity of stable equilibrium still persists.

Similarly, for the modified Sherman model (6), when starting from the rare attractor and introducing small noise intensity in the system, the trajectory fluctuates in the vicinity of the equilibrium, and can not reach bursting attractor (Fig. 4 a),  $D = 0.02$ ). The stationary distribution in this case is also unimodal, concentrated in the vicinity of stable equilibrium point (Fig. 4 c)). However, in the presence of increased noise intensity, the situation significantly changes: initially, the system states in the vicinity of the stable equilibrium ( $t = (0 - 15)$ ), after which the system transits to the bursting attractor and does not switch back (Fig. 4 b)). This absence of switching between the two attractors in the presence of noise could be a result of: (i) the small basin of attraction of the stable equilibrium; (ii) the equilibrium point is located far enough from fast-slow manifolds where the bursting attractor is situated making the switching unlikely; and (iii) noise influences the variable representing the membrane potential of the cell  $V$ . However, the equilibrium point is distanced in direction of the variable  $S$ , thus the noise fluctuations can not induce a shift of the phase space trajectory into the basin of attraction of the equilibrium point. This means that when the bursting attractor is hidden and coexists with a rare attractor, stochastic switching can not be induced between both stable attractors.

We next estimated the possibility to realise the stochastic switching between the coexisting attractors as a function of noise intensity ( $D$ ). In Fig. 5, the residence time that the phase space trajectory spends in the vicinity of the stable equilibrium is plotted as a ratio to the total time series length,  $\rho = \frac{T_{fluct}}{T}$ . As shown before, for small noise intensities that phase space trajectory resides in the vicinity of the stable equilibrium for both models ( $\rho = 1$ ). With increase of  $D$  however, a threshold is observed for which switching to the bursting attractor occurs ( $\rho \neq 1$ ). For the first model, this threshold is significantly less than for the second, and is connected with the size of the basin of attraction of the equilibrium point (which is smaller for the leech neuron model). After the trajectories cross this threshold, there is still a range of noise intensities for which they will still switch between the bursting and the equilibrium state, and this time approximately corresponds to the probability to reach equilibrium for randomly initial conditions. In the Sherman model however, the transition to the bursting attractor after the threshold is irreversible ( $\rho = 0$ ).

## 4 Conclusions

The stochastic switching behavior of bistable system where coexistence of bursting hidden, or self-excited attractor with rare attractor exist are shown. We demonstrate that noise can induce significantly different dynamical behavior, depending on the structure of the phase space and the positioning of the coexisting attractors to each other. In the case when silent state and bursting attractor are distanced from each other in the direction of dynamical variable which are not influenced by noise, no stochastic switching will be observed between the coexisting attractors. An irreversible jump from the rare silent state to the bursting attractor will be observed for low noise

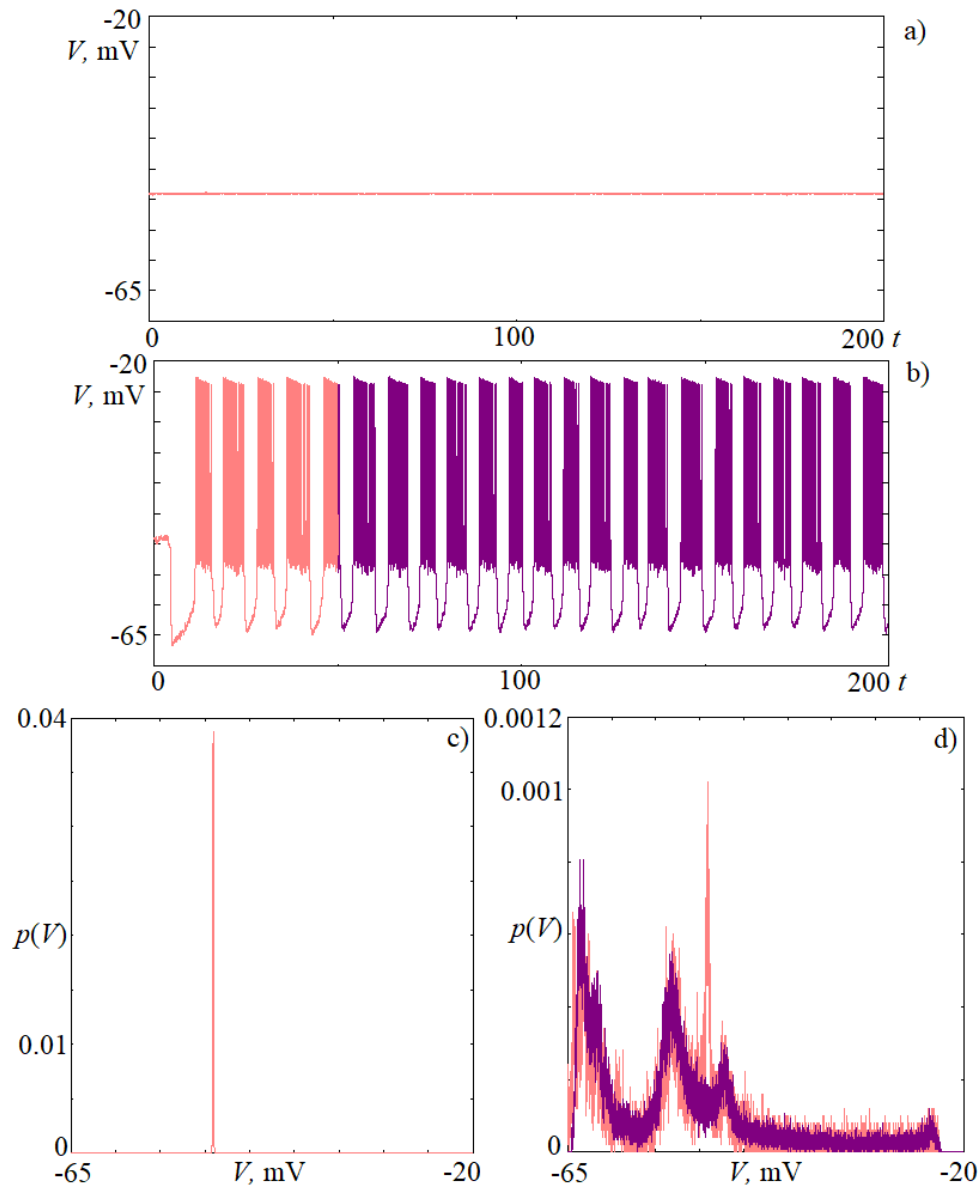


**Fig. 4.** a) and b) Time series of the fast variable  $V$ , and the corresponding c) and d) stationary distribution for model (6) with and different noise intensity: a), c)  $D = 0.017$ ; b), d)  $D = 0.5$ .

intensities. In the case when the dynamical variables are not spatially separated on the manifolds, stochastic switching between both attractors will be observed.

## 5 Acknowledgements

In this research the study of hidden attractors was supported by the Russian Science Foundation project 14-21-00041. NVS thanks also DAAD for the financial support her scientific visit MPI MP in 2016 (Project Number 18.694.2016).

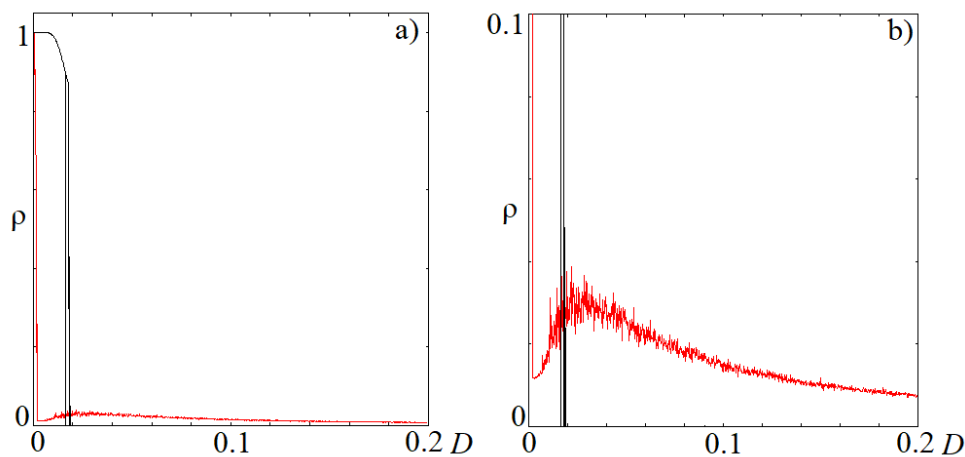


**Fig. 5.** Residence time in the silent state as a function of the noise intensity  $D$ . The red line corresponds to the model (1), and the black line - to the model (6). b) represents a zoomed region from a).

## References

1. Heyward P., Ennis M., Keller A., & Shipley M. T., *Journal of Neuroscience* **21**, (2001) 5311-5320.
2. Pomerening J.R., Sontag E.D., & Ferrell J.E., *Nature cell biology* **5**, (2003) 346-351.
3. Loewenstein Y., Mahon S., Chadderton P., Kitamura K., Sompolinsky H., Yarom Y., & Häusser M., *Nature neuroscience* **8**, (2005) 202-211.
4. Kelso J.A.S., *Phil. Trans. R. Soc. B* **367**, (2012) 906-918.
5. Pisarchik A.N., Feudel U., *Physics Reports* **540**, (2014) 167-218.
6. Kussell E., & Leibler S. *Science*, **309**, (2005) 2075-2078.
7. Acar M., Mettetal J. T., & Van Oudenaarden A. *Nature genetics*, **40**, (2008) 471-475.
8. Koseska A., Zaikin A., García-Ojalvo J., & Kurths J. *Physical Review E* **75** (2007) 031917.
9. Koseska A., Zaikin A., Kurths J., García-Ojalvo J., *PLoS ONE* **4** (2009) e4872.
10. Suzuki N., Furusawa C., & Kaneko K. *PloS one* **6** (2011) e27232.
11. Cymbalyuk G., *Phys.Rev.E* **84**, (2011) 041910
12. Malashchenko T., Shilnikov A., & Cymbalyuk G., *PloS One* **6**, (2011) e21782.
13. Malashchenko T., Shilnikov A., & Cymbalyuk G., *Phys.Rev.E* **84**, (2011) 041910.
14. Barnett W., O'Brien G., Cymbalyuk G., *Journal of Neuroscience Methods* **220**, (2013) 179-189.
15. Marin B., Barnett W.H., Doloc-Mihu A., Calabrese R.L., Cymbalyuk G., *PloS One* **9**, (2013) e1002930.
16. Cymbalyuk G. *Multistability in Neurodynamics: Overview*. In: Jaeger D., Jung R. (eds) *Encyclopedia of Computational Neuroscience* (Springer, New York, NY, 2015).
17. Sherman A., *Bulletin of mathematical biology*, **56** (1994) 811-835.
18. Jalife J., Antzelevitch C., *Science* **206**, (1979) 695-697.
19. Hodgkin A. L., Huxley A. F. *The Journal of physiology* **117**, (1952) 500-544.
20. Moss F., McClintock P. V. E. (ed.). *Noise in Nonlinear Dynamical Systems: Theory of noise induced processes in special applications* (Cambridge University Press, 1989).
21. Kaneko K., *Physical Review Letters* **78**, (1997) 2736.
22. Leonov G.A., Kuznetsov N.V., *Int.J.Bif.Chaos* **23**, (2013) 1330002.
23. Dudkowskii D., Jafari S., Kapitaniak T., Kuznetsov N.V., Leonov G.A., Prasad A. *Physics Reports* **637**, (2016) 1-50.
24. Raj A., van Oudenaarden A., *Cell* **135**, (2008) 216-226.
25. Wells D.K., Kath W.L., & Motter A.E., *Phys.Rev.X* **5** (2015) 031036.

26. Brezetskyi S., Dudkowski D., & Kapitaniak T., *Eur.Phys.J.Special Topics* **224**, (2015) 1459-1467.
27. Stankevich N.V., Mosekilde E., *CHAOS* **27**, (2017) 123101.
28. Hill A.A., Lu J., Masino M.A., Olsen O.H., & Calabrese R.L., *Journal of computational neuroscience* **10**, (2001) 281-302.
29. Zakharova A., Vadivasova T., Anishchenko V., Koseska A., Kurths J. *Phys.Rev.E* **81**, (2010) 011106.
30. Kamal N.K., Varshney V., Shrimali M.D., Prasad A., Kuznetsov N.V., & Leonov G.A., *Nonlinear Dynamics*, **91**, (2018) 1-6.